

Supplement of Biogeosciences, 13, 3607–3618, 2016  
<http://www.biogeosciences.net/13/3607/2016/>  
doi:10.5194/bg-13-3607-2016-supplement  
© Author(s) 2016. CC Attribution 3.0 License.



Biogeosciences  Open Access

*Supplement of*

**New strategies for submicron characterization the carbon binding of reactive minerals in long-term contrasting fertilized soils: implications for soil carbon storage**

**Jian Xiao et al.**

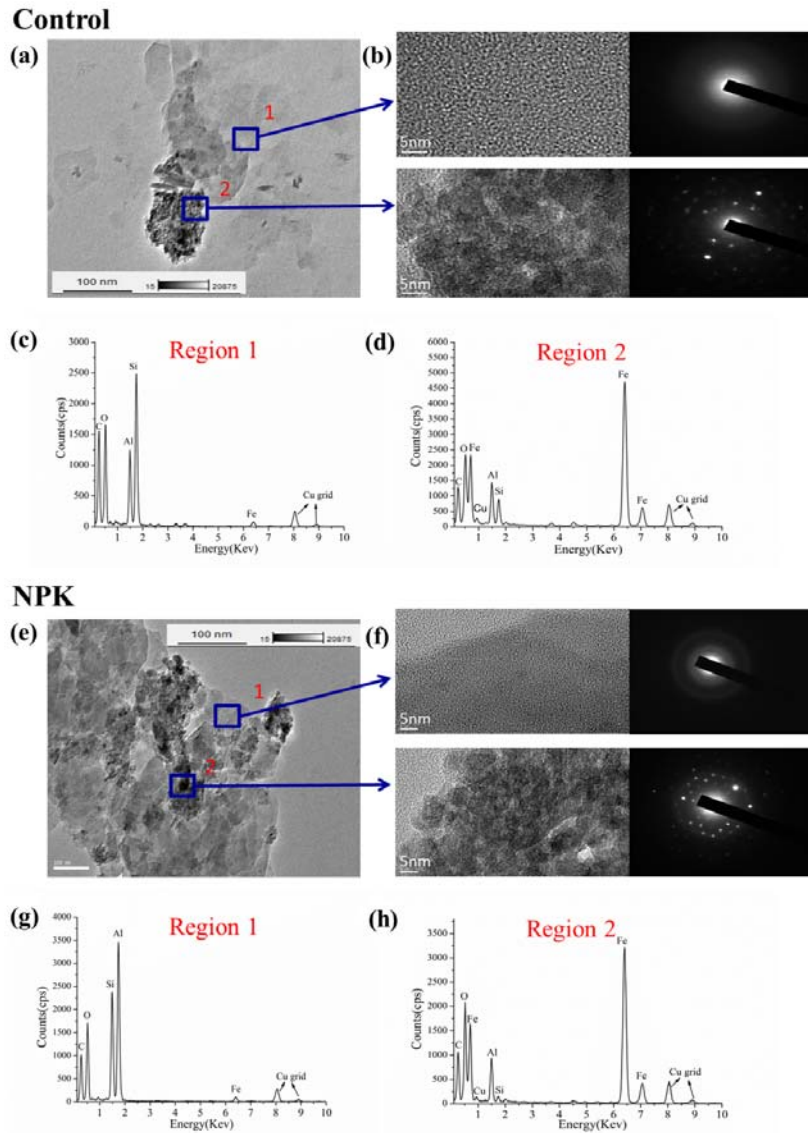
*Correspondence to:* Guanghui Yu ([yuguanghui@njau.edu.cn](mailto:yuguanghui@njau.edu.cn))

The copyright of individual parts of the supplement might differ from the CC-BY 3.0 licence.



**Fig. S1.** Field fertilization layout and extracted soil (Ferralic Cambisol) colloids from three 24-year (1990-2014) long-term fertilization treatments. Control, no fertilization; NPK, chemical nitrogen, phosphorus and potassium fertilization; NPKM, chemical

15 NPK plus swine manure fertilization.



20 **Fig. S2.** High-resolution transmission electron microscopy (HRTEM) images of highly reactive minerals in colloids extracted from soils (Ferralic Cambisol) after 24-year long-term (1990-2014) no fertilization control (a-d) and NPK fertilization

(e-h). (a and e), TEM images; (b and f), HRTEM images and selected area electron diffraction (SAED) patterns of the two regions indicated by the blue squares, showing

25 that the black region is a complete crystalline, while the grey region is amorphous;

(c-d and g-h) energy dispersive X-ray analysis (EDX) images of the region 1 and region 2. Control, no fertilization; NPK, chemical nitrogen, phosphorus and potassium fertilization.

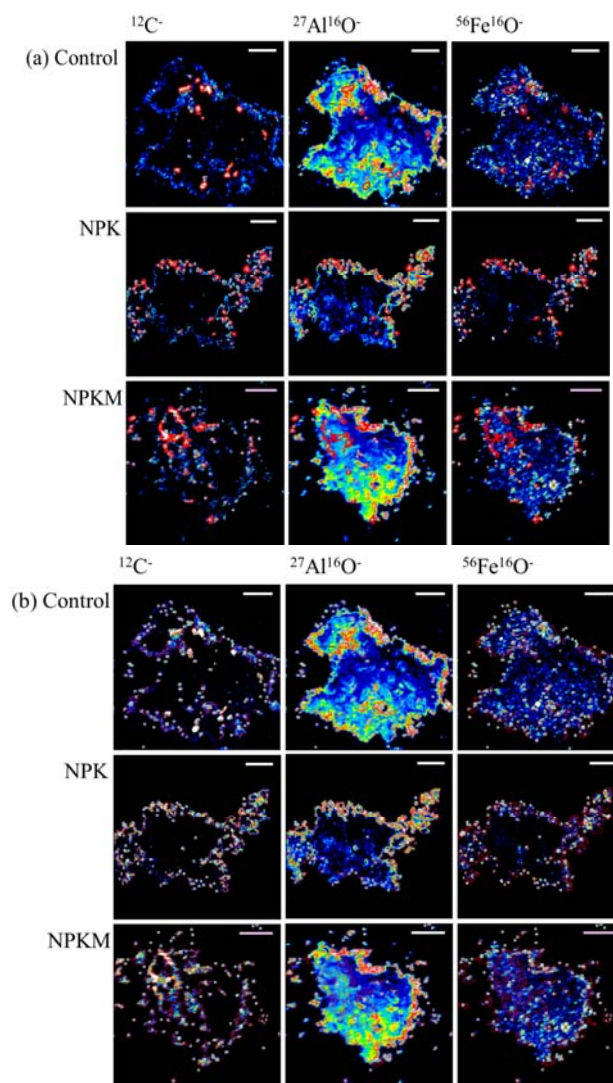


**Fig. S3.** Region of interests (ROIs) (circled by red line) of  $^{12}\text{C}^-$ ,  $^{27}\text{Al}^{16}\text{O}^-$  and  $^{56}\text{Fe}^{16}\text{O}^-$  presenting on the NanoSIMS images in colloids extracted from soil (Ferralic Cambisol) after 24-year (1990-2014) long-term fertilization treatments. NanoSIMS images of (a) the  $^{12}\text{C}^-$  rich ROIs of  $^{12}\text{C}^-$ ,  $^{27}\text{Al}^{16}\text{O}^-$  and  $^{56}\text{Fe}^{16}\text{O}^-$  (b) the  $^{12}\text{C}^-$  less rich ROIs of  $^{12}\text{C}^-$ ,  $^{27}\text{Al}^{16}\text{O}^-$  and  $^{56}\text{Fe}^{16}\text{O}^-$ . Control, no fertilization,  $28 \times 28 \mu\text{m}^2$ ; NPK, chemical nitrogen, phosphorus and potassium fertilization,  $30 \times 30 \mu\text{m}^2$ ; NPKM, chemical NPK plus swine manure fertilization,  $25 \times 25 \mu\text{m}^2$ . Note that the color intensity calibration bar displayed in the chemical maps corresponds to the relative concentrations of individual elements, but cannot be used to compare one element to another. Bar =  $5 \mu\text{m}$ .

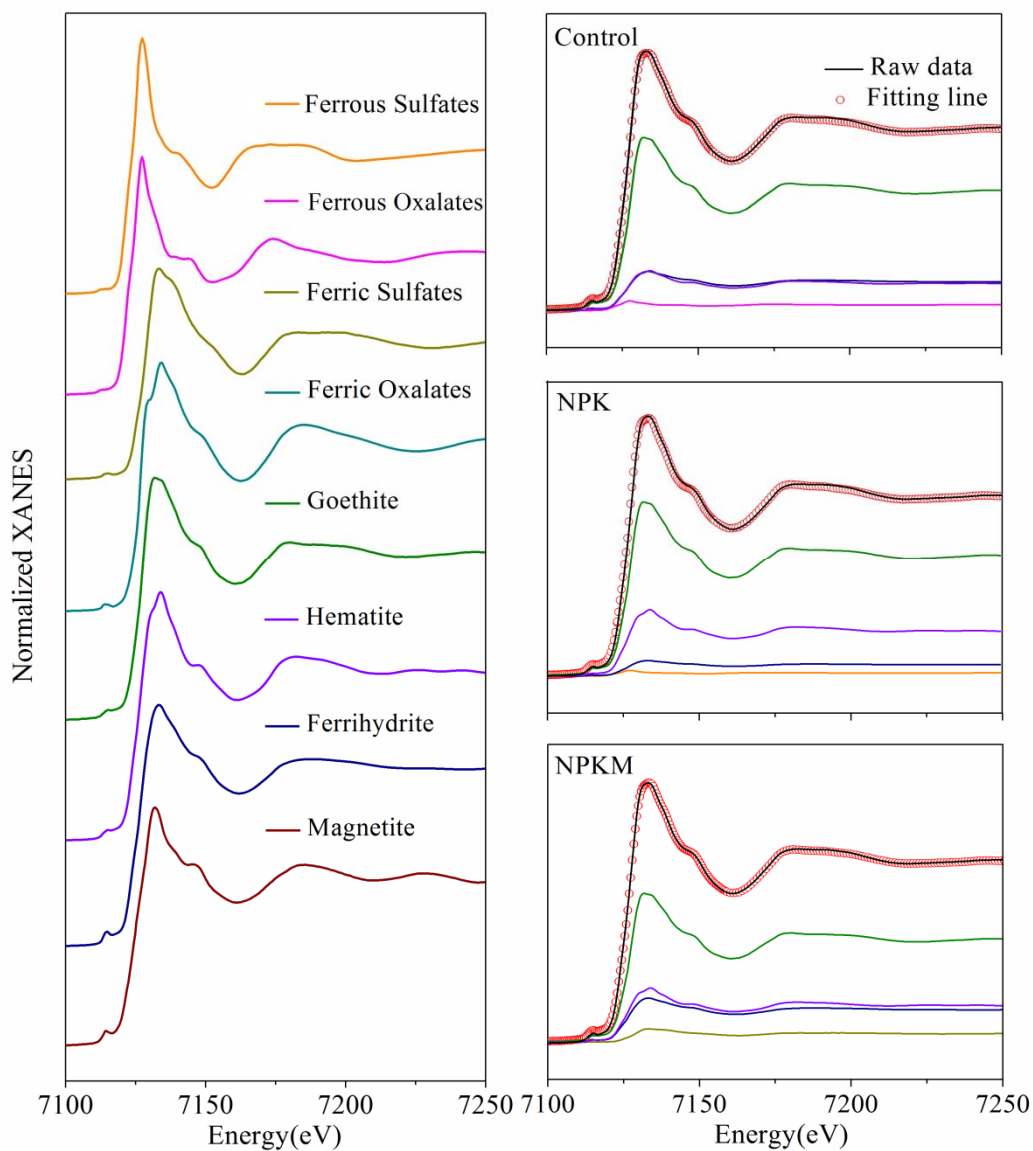


**Fig. S4.** Fe K-edge XANES spectra of reference materials and soil colloids from soil (Ferralic Cambisol) after three contrasting long-term (1990-2014) fertilization treatments. The scattered circles represent the linear combination fitting (LCF) results of the sample spectra. Control, no fertilization; NPK, chemical nitrogen, phosphorus and potassium fertilization; NPKM, chemical NPK plus swine manure fertilization.

48 **Table S1. Annual fertilization rates between 1990 and 2014 in Qiyang, China <sup>a</sup>.**

Treatment	Wheat				Corn			
	N (kg ha <sup>-1</sup> )	P (kg ha <sup>-1</sup> )	K (kg ha <sup>-1</sup> )	Swine manure (Mg ha <sup>-1</sup> )	N (kg ha <sup>-1</sup> )	P (kg ha <sup>-1</sup> )	K (kg ha <sup>-1</sup> )	Swine manure (Mg ha <sup>-1</sup> )
	Control	0	0	0	0	0	0	0
NPK	27	16	31	0	63	37	73	0
NPKM	90	16	31	10-15	210	37	73	25-35

<sup>a</sup>Note: N fertilizer was as urea, P as calcium superphosphate, K as KCl. Swine manure was calculated in fresh weight. Control, no fertilization; NPK, chemical nitrogen, phosphorus and potassium fertilization; NPKM, chemical NPK plus swine manure fertilization.

50 **Table S2. Quantification of  $^{12}\text{C}^-$  rich ( $^{12}\text{C}^-$ -R) and  $^{12}\text{C}^-$  less-rich ( $^{12}\text{C}^-$ -LR) region of interests (ROIs) <sup>a</sup>**

	$^{12}\text{C}^-$ Rich ROIs				$^{12}\text{C}^-$ Less-Rich ROIs		
	Replicates	ROIs	ROIs Area	Intensity	ROIs	ROIs Area	Intensity
Treatment	Number	Number	/Total area (%)	(Pixel)	Number	/Total area (%)	(Pixel)
Control	8	312	7.47	>90	457	40.18	40-90
NPK	6	567	10.80	>90	532	27.64	40-90
NPKM	6	479	8.23	>50	596	37.99	30-50

<sup>a</sup> Note: Control, no fertilization; NPK, chemical nitrogen, phosphorus and potassium fertilization; NPKM, chemical NPK plus swine manure fertilization.

51 **Table S3. Fe mineral standards used in the fitting of Fe K-edge XANES spectra**

<b>Fe mineral standards</b>	<b>Mineral type</b>	<b>Chemical formula</b>	<b>Origin</b>	<b>References</b>
<b>Ferrous sulfate</b>	Inorganic ferrous oxides	$\text{FeSO}_4 \cdot 7\text{H}_2\text{O}$	Aladdin, CAS:7782-63-0	-
<b>Ferrous oxalate</b>	Organic ferrous oxides	$\text{FeC}_2\text{O}_4 \cdot 2\text{H}_2\text{O}$	Aladdin, CAS:6047-25-2	-
<b>Ferric sulfate</b>	Inorganic ferric oxides	$\text{Fe}_2(\text{SO}_4)_3 \cdot 2\text{H}_2\text{O}$	Aladdin, CAS:10028-22-5	-
<b>Ferric oxalate</b>	Organic ferric oxides	$\text{Fe}_2(\text{C}_2\text{O}_4)_3 \cdot 5\text{H}_2\text{O}$	Aladdin, CAS: 2944-66-3	-
<b>Goethite</b>	Iron Oxide	$\alpha\text{-FeOOH}$	Synthetic	Schwertmann & Cornell (2007b)
<b>Hematite</b>	Iron Oxide	$\alpha\text{-Fe}_2\text{O}_3$	Synthetic	Yen et al. (2002) Schwertmann & Cornell (2007c)
<b>Ferrihydrite</b>	Iron Oxide	$\text{Fe}_5\text{HO}_8 \cdot 4\text{H}_2\text{O}$	Synthetic	Michelet al. (2007) Schwertmann & Cornell (2007a)
<b>Maghemite</b>	Iron Oxide	$\gamma\text{-Fe}_2\text{O}_3$	Synthetic	Wang et al. (2008) Schwertmann & Cornell (2007d)



52 **References**

- 53 Michel, F.M., Ehm, L., Antao, S.M., Lee, P.L., Chupas, P.J., Liu, G., Strongin, D.R.,  
54 Schoonen, M.A.A., Phillips, B.L., and Parise, J.B.: The structure of ferrihydrite, a  
55 nanocrystalline material, *Science*, 316, 1726-1729, 2007.
- 56 Mueller, C.W., Kölbl, A., Hoeschen, C., Hillion, F., Heister, K., Herrmann, A.M., and  
57 Kögel-Knabner, I.: Submicron scale imaging of soil organic matter dynamics  
58 using NanoSIMS-From single particles to intact aggregates, *Org. Geochem.*, 42,  
59 1476-1488, 2012.
- 60 Schwertmann, U., and Cornell, R.M.: Ferrihydrite, *Iron Oxides in the Laboratory*,  
61 Wiley-VCH Verlag GmbH, pp. 103-112, 2007a.
- 62 Schwertmann, U., and Cornell, R.M.: Goethite, *Iron Oxides in the Laboratory*,  
63 Wiley-VCH Verlag GmbH, pp. 67-92, 2007b.
- 64 Schwertmann, U., and Cornell, R.M.: Hematite, *Iron Oxides in the Laboratory*,  
65 Wiley-VCH Verlag GmbH, pp. 121-134, 2007c.
- 66 Schwertmann, U., and Cornell, R.M.: Maghemite, *Iron Oxides in the Laboratory*,  
67 Wiley-VCH Verlag GmbH, pp. 141-142, 2007d.
- 68 Wang, X.G., Liu, C.S., Li, X.M., Li, F.B., and Zhou, S.G.: Photodegradation of  
69 2-mercaptobenzothiazole in the  $\gamma$ -Fe<sub>2</sub>O<sub>3</sub>/oxalate suspension under UVA light  
70 irradiation, *J. Hazard. Mater.*, 153, 426-433, 2008.
- 71 Yen, F.S., Chen, W.C., Yang, J.M., and Hong, C.T.: Crystallite size variations of  
72 nanosized Fe<sub>2</sub>O<sub>3</sub> powders during  $\gamma$ - to  $\alpha$ -phase transformation, *Nano Lett.*, 2,  
73 245-252, 2002.